



Fluid inclusion evidence on the direct exsolution of magmatic brines from a granite intrusion beneath the eastern sector of Larderello geothermal field (Italy)

Paolo Fulignati *

Dipartimento di Scienze della Terra, Via S. Maria 53, 56126 Pisa, Italy

ARTICLE INFO

Submitted: April 2017

Accepted: August 2017

Available on line: September 2017

* Corresponding author:
paolo.fulignati@unipi.it

DOI: 10.2451/2017PM720

How to cite this article:
Fulignati P. (2017)
Period. Mineral. 86, 201-211

ABSTRACT

This work is based on a fluid inclusion investigation on two core samples (sampled at 3017 m and 4150 m of depth) of a granite intrusion drilled by the Travale 1 sud geothermal well, in the eastern sector of Larderello geothermal field. Fluid inclusion data demonstrate that the earliest fluids circulating in the intrusion were high-temperature brines exsolved directly from the crystallizing magma during its ascent in the shallow crust. The progressive release of magmatic fluids from the crystallizing granitic magma probably occurred under confining lithostatic pressure of about 200 MPa. Two phase fluid inclusions represent the hydrothermal meteoric water-dominated fluids that penetrated in the granite after opening of the system, induced by cooling and consequent transition from ductile behaviour to brittle fracturing. Type 1b two phase fluid inclusions, having temperature of homogenization that agree well with down-hole measured temperatures, may be considered to approximate the fluid that is actually circulating in the granite in recent times.

Keywords: fluid inclusions; magmatic fluids; hydrothermal system; Larderello geothermal field.

INTRODUCTION

The Larderello geothermal field is one of the few vapour-dominated geothermal system in the world and has been extensively exploited for several decades for power production. It represents the most striking feature of the active hydrothermal activity that interests southern Tuscany. This important hydrothermal activity is strictly related to the very high heat flow (120 to more than 1000 mWm⁻², Baldi et al., 1995), which characterizes southern Tuscany. The high heat flow values are due to the Neogene magmatism of the Tuscan magmatic Province and crustal thinning (Marinelli, 1963, Marinelli et al., 1993; Serri et al., 1993; Mongelli et al., 1998; Dini et al., 2005). In particular, geological, geophysical and geochemical data indicate the presence of shallow intrusive bodies (2-5 km) beneath the Larderello geothermal field, belonging to a composite batholith (Gianelli et al., 1997), which was built by emplacement of multiple intrusions of granitic

magmas between 3.8 and 1.3 Ma (Villa et al., 1997; Dini et al., 2005). In the last decades, Larderello composite batholith and the associate thermometamorphic and metasomatic aureola have been penetrated by several deep geothermal wells (Barelli et al., 2000; Boyce et al., 2003; Dini et al., 2005; Bertini et al., 2006). Furthermore, geophysical data support the existence of a still partially molten magmatic body below Larderello (Gianelli et al., 1997), which is considered to be responsible of the very high thermal anomaly of the area, reaching values in excess of 300 °C·km⁻¹ (Baldi et al., 1995).

Several studies have been carried out on the hydrothermal fluid evolution in the subsoil of Larderello geothermal field, revealing a complex system from an early stage, dominated by magmatic and thermometamorphic fluids, to the present-day stage in which fluids of meteoric origin are dominant (Belkin et al., 1985; Valori et al., 1992; Cathelineau et al., 1994; Ruggieri and Gianelli,

1999; Ruggieri et al., 1999; Boyce et al., 2003; Boiron et al., 2007). In particular, the occurrence of magmatic fluids in the early stage of hydrothermal activity has been postulated by Cathelineau et al. (1994) on the basis of a study on hypersaline fluid inclusions, found in quartz crystals of hornfels and leucogranite dykes from the deeper portions of the Larderello geothermal system.

This paper is focused on the hydrothermal fluid evolution in a granite intrusion drilled by "Travale 1sud" (Trav. 1s) deep geothermal well (eastern sector of Larderello geothermal field), through a fluid inclusion study. Particular emphasis will be devoted to show, for the first time at Larderello, clear evidences on the direct exsolution of hypersaline magmatic brines from the granite intrusion. This assumes a particular interest because, as stated above, the involvement of fluids exsolved from crystallizing granite magmas, during the early stage of evolution of Larderello geothermal system, has been only deduced in previous works (Valori et al., 1992; Cathelineau et al., 1994), but direct evidences of magmatic fluid exsolution were never reported before. The pressure-temperature conditions of fluid exsolution will be furthermore discussed as well as the transition to the hydrothermal meteoric water-dominated stage.

TRAVALE 1SUD GEOTHERMAL WELL LITHOSTRATIGRAPHY

The Trav 1s geothermal well is located in the eastern sector of Larderello geothermal field (Figure 1) on 455 m of dolomitic limestone and anhydrite of the Tuscan Nappe. The borehole then cuts Paleozoic phyllite complex, made up of phyllites and phyllitic sandstone with intercalation of anhydrites and limestone, down to 1630m. From 1630m down to 2680 m the well passes through the thermometamorphic complex, which consists of thermometamorphic phyllites (hornfels) intercalated by skarn and thin veins of granitic composition (Figure 2). At 2680 m the thermometamorphic complex is in contact with a granite intrusion, which is cut to the bottom of the hole at 4150 m (Barelli et al., 2000).

The intrusion is a leucogranite with a mineral association of: quartz - plagioclase - K-feldspar - biotite - cordierite - tourmaline. Leucogranite shows fine to medium-grained disequigranular texture, with perthitic feldspar phenocrysts ranging from 1 to 3 cm in size. K-feldspar also occurs as small grains (300-600 μm), these latter strictly associated with fine-grained plagioclase (150-300 μm). Fine-grained red brown biotite (150-300 μm) and rare pinitised cordierite also occur.

The two core samples are characterized by pervasive hydrothermal alteration carried out by a mineralogical assemblage made up of chlorite + illite + albite \pm adularia \pm hydrothermal biotite \pm calcite. Chlorite partially substitutes magmatic biotite whereas albite and illite

are generally found as alteration of plagioclase and K-feldspar. No difference of hydrothermal alteration paragenesis was observed with increasing depth, with the exception of a general increase of chlorite as alteration of magmatic biotite.

ANALYTICAL METHODS

This study was carried out on two core samples from the Trav. 1s geothermal well sampled at 3017 m and 4150 m of depth. The thermometric behaviour of fluid inclusions was studied using doubly polished thin sections on a Linkam THMS 600 heating-freezing stage (Dipartimento di Scienze della Terra, Univ. Pisa). The precision and accuracy of the microthermometric measurements is estimated at ± 2 °C at 398 °C controlled by the melting point of $\text{K}_2\text{Cr}_2\text{O}_7$, ± 0.1 at 0 °C and ± 0.2 at -56.6 °C controlled by using certified pure water and CO_2 -bearing synthetic fluid inclusions (Synthetic Fluid Inclusion Reference Set, Bubbles Inc., USA). Salinity estimates were determined from the last melting temperatures of ice (Bodnar, 1993) and from halite melting temperatures (Sterner et al., 1988). Eutectic temperatures were used to constrain overall composition of the solutions by comparison with published data for various salt-water systems (Crawford, 1981; Shepherd et al., 1985).

RESULTS

Petrography and texture of fluid inclusions

Fluid inclusions hosted within quartz crystals have been studied in intrusive rock cored at 3017 and 4150 m of depth. The inclusions observed were assigned a probable primary or secondary origin according to the criteria of Roedder (1984) and Goldstein (2003). All descriptions strictly refer to fluid inclusion assemblages (FIAs, Goldstein and Reynolds, 1994), avoiding single isolated fluid inclusions, and the types of fluid inclusions in each FIA were noted. In general, Type 1 (a and b), Type 2 and Type 3 (a and b) fluid inclusions that belong to an individual FIA, show consistent microthermometric data suggesting that post-trapping processes did not significantly affect the inclusions. The size of the analyzed fluid inclusions is in the range 5-30 μm . Several fluid inclusion types were determined on the basis of microscopic and microthermometric data. Microscopic observation at room temperature revealed three main types of fluid inclusions (Figure 3 a,b,c):

Type 1: two-phase liquid-rich (L+V) fluid inclusions. Two sub-populations can be distinguished on the basis of petrographic observation: Type 1a and Type 1b. Type 1a inclusions are secondary in origin and are characterized by a scarce variability in the vapour/liquid ratio (the vapour bubble fills 20-30% of the inclusions). Type 1b inclusions are secondary in origin and often occur in elongated

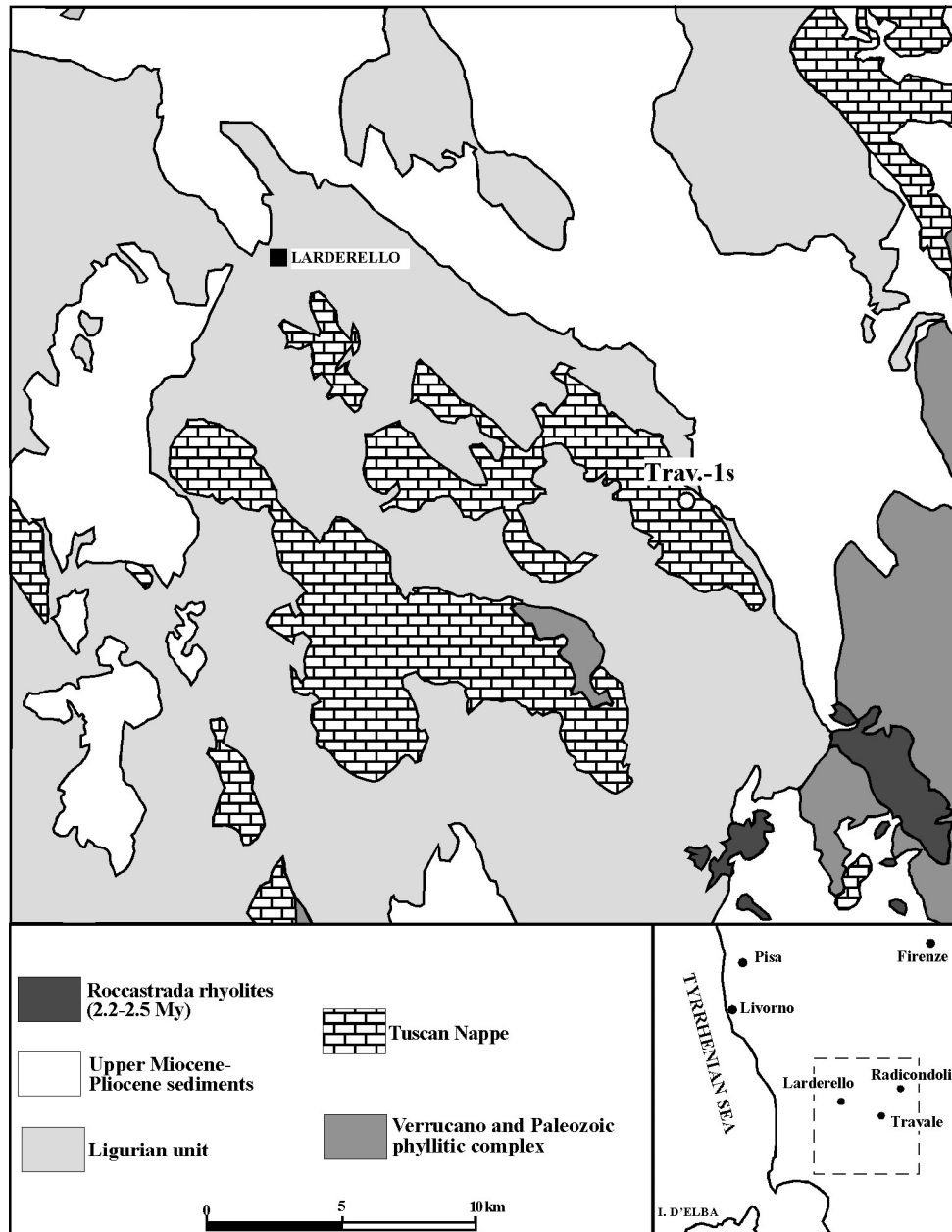


Figure 1. Geological sketch map of the Larderello geothermal field area with location of Trav. 1s geothermal well (from Gianelli et al., 1978, modified).

trails that cut across the quartz crystals. In Type 1b fluid inclusions the vapour/liquid ratio is more variable than in Type 1a inclusions, with the vapour bubble that fills 15-40% of the inclusions. The petrographic relationships between the two sub-populations of Type 1 fluid inclusions are not clear, as a consequence we cannot make an unequivocal interpretation of the timing of entrapment.

Type 2: two-phase vapour-rich (V+L) fluid inclusions. Secondary vapour-rich fluid inclusions were found only in the core sample at 3017m of depth of Trav-1s

well. No clear relationships are observed between Type 2 inclusions and the other fluid inclusion generations. Type 2 inclusions occur in trails filled only by this type of inclusions (Figure 3b), and only very rarely they are associated with Type 1a fluid inclusions. In many of these inclusions the liquid phase is not visible under the microscope probably because the liquid phase is scarce.

Type 3: multiphase liquid-rich (L+V+daughter minerals) fluid inclusions were found only in the core sample at 4150 m of depth of Trav-1s well. Daughter

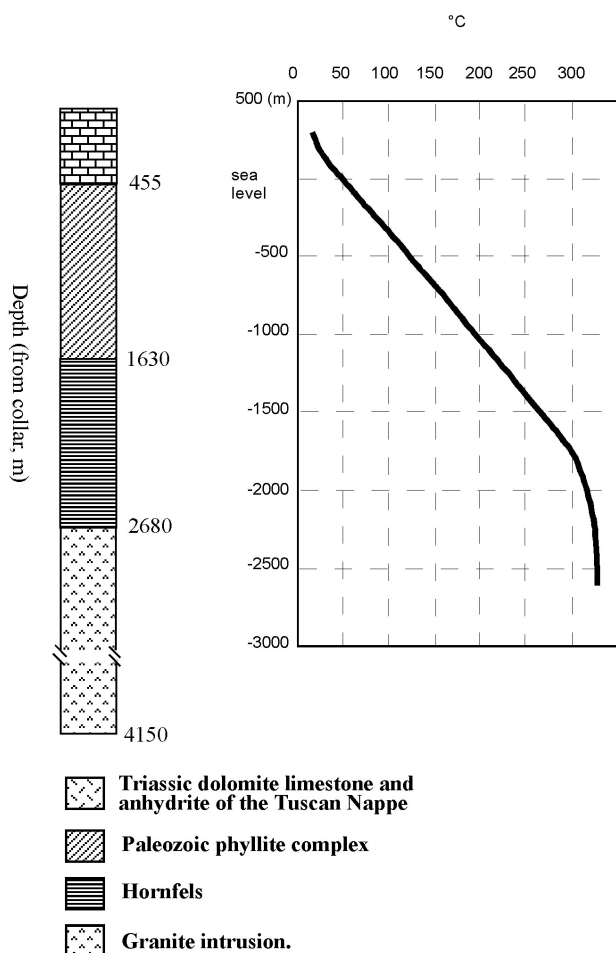


Figure 2. Schematic lithostratigraphic column and thermal profile of the Trav. 1s geothermal well (data from Barelli et al., 2000).

minerals are represented by halite \pm sylvite \pm other solids that have tabular and elongated habits and in some cases show birefringence. Opaque mineral are sometimes observed.

Two sub-populations of multiphase fluid inclusions are distinguished on the basis of petrographic observation: Type 3a and Type 3b. Type 3a fluid inclusions are commonly found in trails elongated in the direction of growth of quartz crystals or in isolated clusters (Figure 3c), and hence bear an unambiguous primary origin (Goldstein, 2003). Type 3b inclusions occur in planar arrays that cut across the host crystals and in several cases cut also Type 3a trails, suggesting a secondary origin (Figure 3c).

Microthermometric results

The results of the microthermometric investigation are reported in Figure 4 and in Table 1. Fluid inclusions

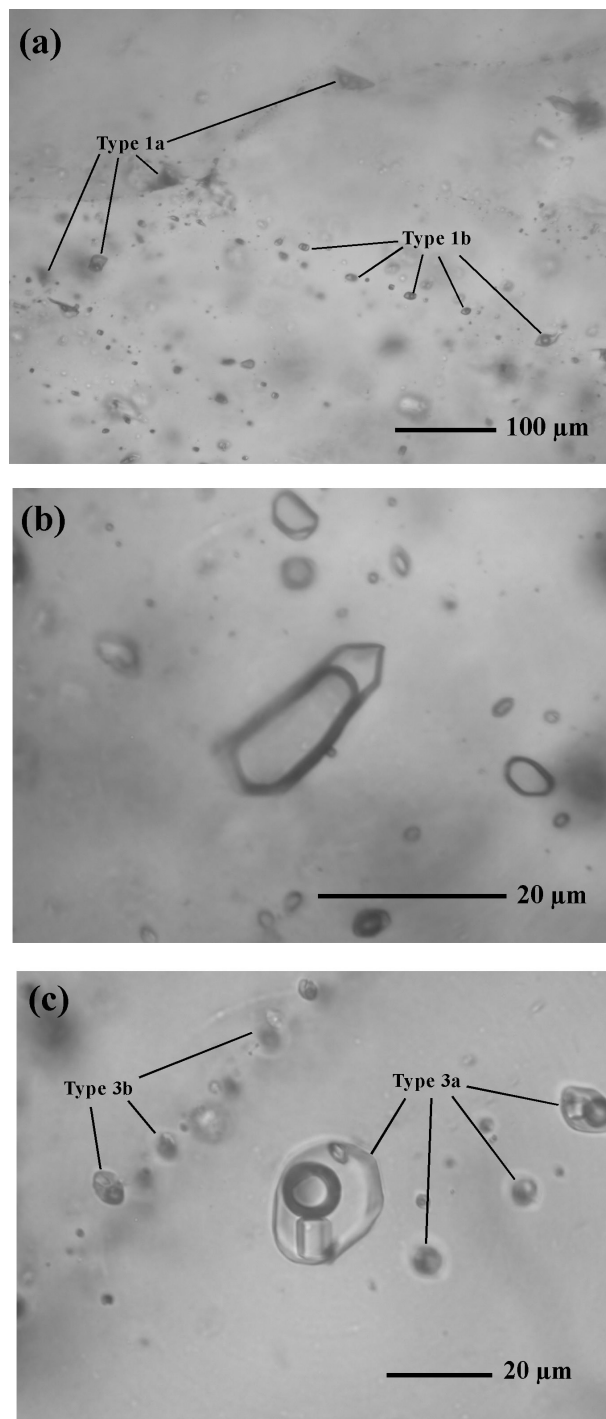
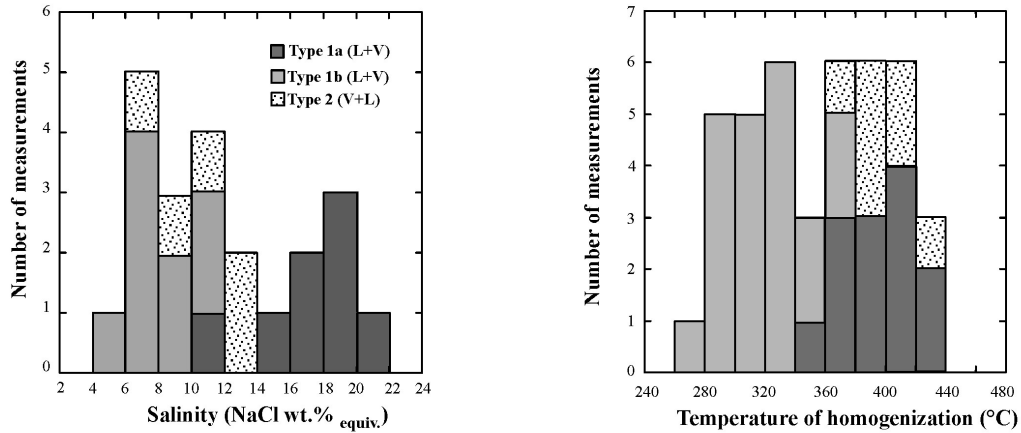


Figure 3. Microphotographs of the different fluid inclusion types: (a) Type 1a and Type 1b two-phase (L+V) fluid inclusions; (b) Type 2 two-phase (V+L) fluid inclusions; (c) primary Type 3a multiphase (L+V+daughter minerals) fluid inclusions with a secondary trail of Type 3b multiphase (L+V+daughter minerals) fluid inclusions.

Core at 3017m



Core at 4150m

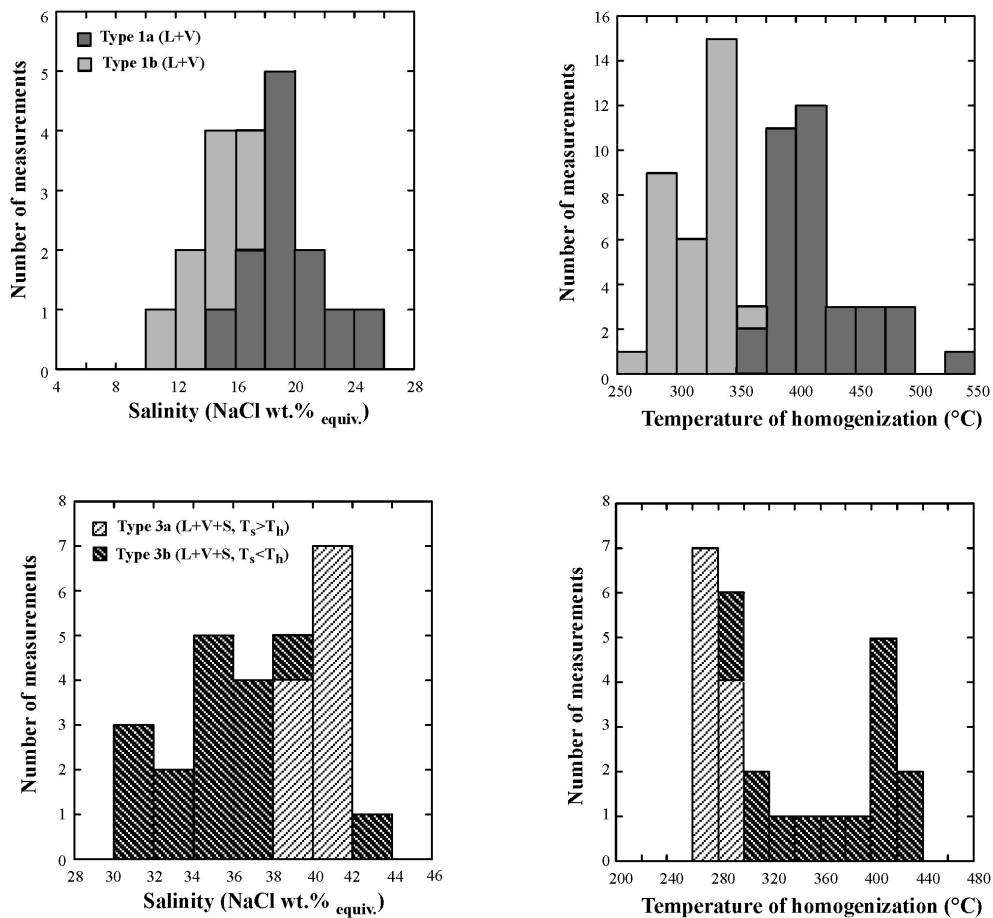


Figure 4. Histograms of the temperature of homogenization and salinities of the fluid inclusions studied in Travale 1sud well at 3017 m and 4150 m of depth. N = number of measurements.

Table 1. Summary of fluid inclusion data.

Well	Depth (m)	Inclusion type	T_e	T_{mi}	T_s	Salinity ¹	T_h
Trav. 1s	3017	Type 1a	-30.0/-54.2°C [11]	-7.8/-18.0°C [8]		11.5÷21.0 [8]	340÷440°C [13]
		Type 1 - Two phase liquid-rich fluid inclusions (L+V)	-41.0°C	-14.8°C		19	400°C
		Type 1b	-26.4/-53.0°C [8]	-3.6/-8.0°C [9]		5.9÷11.7 [9]	260÷380°C [21]
			-40.0°C	-4.8°C		7	340°C
		Type 2 - Two phase vapour-rich fluid inclusions (V+L)	nd	-4.4/-9.6°C [5]		7.0÷13.5 [5]	360÷440°C [7]
				-8.5°C		13	390°C
		Type 1a	-32.1/-54.6°C [4]	-10.2/-23.6°C [12]		14.2÷24.7 [12]	375÷550°C [33]
		Type 1 - Two phase liquid-rich fluid inclusions (L+V)		-15.5°C		19	410°C
		Type 1b	-31.0/-51.5°C [3]	-6.9/-13.4°C [8]		10.4÷17.3 [8]	250÷350°C [31]
				-11.1°C		15	335°C
	4150	Type 1a	-45.1/-55.5°C [5]		302÷340°C [11]	38.0÷42.0 [11]	260÷300°C [33]
Type 3 - Multiphase liquid-rich fluid inclusions (L+V+1 or more salts)				335°C	41	270°C	
		Type 1b	-46.0/-53.5°C [3]		180÷365°C [16]	31.0÷44.0 [16]	280÷440°C [13]
				260°C	35	410°C	

T_e = temperature of first ice melting; T_s = temperature of halite homogenization; [] = number of measurements; T_{mi} = temperature of final ice melting; T_h = temperature of vapor bubble homogenization; bold = modal values; nd = not determined; ¹ = Salinity is reported as wt% NaCl_{equiv}.

freeze to ice upon cooling below -30/-50 °C, as clearly observed by the sudden shrinkage of the vapour bubble. During warming, the temperature of initial melting of ice (eutectic temperature, T_e) was measured for Type 1 and Type 3 inclusions. Because of the small amount of liquid phase, no T_e data could be collected on Type 2 fluid inclusions. The T_e in Type 1 and Type 3 fluid inclusions is always between -35 °C and -50 °C indicating a complex system for the fluids trapped, in which bivalent cations such as Mg²⁺ and Ca²⁺ occur in addition to Na⁺ and K⁺ (Crawford, 1981). Neither liquid CO₂ nor clathrates was observed during cooling runs. Some minor amounts of CO₂ might be however present in the examined fluid inclusions, as a consequence the salinities must be considered as maximum values, since the possible presence of CO₂ can depress the temperature of final ice melting (T_{mi}) by as much as 1.48 °C, corresponding to an overestimation of calculated salinity by up to 2.5 wt% NaCl_{equiv}. (Hedenquist and Henley, 1985).

Core at 3017 m of depth

In the granite at 3017m of depth Type 1a inclusions have a T_{mi} between -7.8° and -18.0 °C with a mode around -14.8 °C, corresponding to salinities of 11.5-21.0 wt% NaCl_{equiv} (mode around 19 wt% NaCl_{equiv}). These inclusions exhibit temperature of homogenization (T_h) in the range 340-440 °C with a mode at about 400 °C. Type 1b fluid inclusions show higher T_{mi} ranging between -3.6° and -8.0 °C with a mode at -4.8 °C. This corresponds to salinities between 5.9 and 11.7 wt% NaCl_{equiv} with a mode around 7 wt% NaCl_{equiv}. The T_h ranges between 260° and 380 °C with a modal value at 330 °C. Type 2 fluid inclusions exhibit T_h in the vapour phase in the range 360-440 °C with a mode around 390 °C. Because of the small amount of liquid phase, after freezing only few T_{mi} were determined. These latter range between -4.4 and -9.6 °C with a fair mode at -8.5, equating to salinities of 7.0 and 13.5 wt% NaCl_{equiv} (mode around 13 wt% NaCl_{equiv}).

Core at 4150 m of depth

At 4150m of depth, Type 1a fluid inclusions show a broad range of T_{mi} (-10.2° to -23.6 °C), corresponding to salinities in the range 14.2-24.7 wt% NaCl_{equiv.} (mode around 19 wt% NaCl_{equiv.}). T_h occurs in the range 375°-550 °C with a mode around 410 °C. In Type 1b fluid inclusions the T_{mi} ranges between -6.9° and -13.4 °C, equating to salinities of 10.4 and 17.3 wt% NaCl_{equiv.} with a mode of about 15 wt% NaCl_{equiv.}. The T_h of Type 1b fluid inclusions are lower than in Type 1a, and are in the range 250°-350 °C with a strong modal value around 335 °C.

In Type 3a multiphase fluid inclusions the total homogenization occurs by halite disappearance (T_s) between 302° and 340 °C with a mode at about 335 °C (salinity in the range 38-42 wt% NaCl_{equiv.}, mode at 41 wt% NaCl_{equiv.}), whilst the T_h in the liquid phase of the bubble is in the range 260°-300 °C with a modal value around 270 °C. The dissolution temperature of sylvite was observed in only few Type 3a inclusions and ranges from 150 °C to 160 °C. Conversely to Type 3a fluid inclusions, in Type 3b fluid inclusions the total homogenization always occurs by bubble disappearance at a temperature ranging from 280 °C and 440 °C with a mode around 410 °C. These inclusions exhibit a T_s between 180° and 365 °C with a mode at about 260 °C corresponding to salinities of 31-44 wt% NaCl_{equiv.}, mode at about 35 wt% NaCl_{equiv.}. No data on dissolution temperature of sylvite was obtained.

DISCUSSION

Evolution of intrusion-related fluids

Fluid inclusion investigation in the granite intrusion of Trav 1s well suggests several events of fluid entrapment during the late stages of granite crystallization, during its cooling and the following hydrothermal event. The occurrence of Type 3 hypersaline fluid inclusions in the core at 4150 m of depth is suggestive of the direct exsolution of a magmatic fluid phase from the granite intrusion. Fluid inclusion observations and microthermometric data suggest that Type 3a fluids were not generated by aqueous fluid immiscibility. The possibility that these saline fluids were generated through formation of immiscible aqueous vapour and brine is unlikely due to the lack of a coexisting population of vapour-rich inclusions that exhibit similar final homogenization temperatures. Phase equilibria constraints require that Type 3a fluid inclusions, homogenized by halite dissolution, trapped fluids in the liquid-stable, vapour-absent field (Cline and Bodnar, 1994). Similar conditions were also reported for the magmatic fluids circulated during early stage of development of the fossil magmatic-hydrothermal system associated to “Botro ai Marmi” Neogene intrusion, outcropping only a few km westward of Larderello geothermal field (Fulignati in prep). To interpret trapping

conditions for these inclusions, microthermometric data of Type 3a inclusions (T_h = 260°-290 °C; T_s =305°-335 °C corresponding to 39 and 41 wt%NaCl_{equiv.}, cluster of data points within oval in Figure 5) are modelled by the simple system NaCl-H₂O, the halite dissolution temperatures can be used to estimate minimum temperature and pressure of entrapment (Figure 6). The slopes of halite liquidus and of the iso- T_h line were determined by using the data of Bodnar (1994) and the Microsoft Excel spreadsheet HOKIEFLINCS-H₂O-NACL (Steele-MacInnis et al., 2012). The iso- T_h lines intersect the liquidus [L(40)+H] at a temperature of about 330 °C and a minimum pressure ranging between 85 to 130 MPa (Figure 6). Such temperature estimate is considered highly unlikely for entrapment related to magmatic fluid and higher temperatures are expected. Trapping of these fluids at higher temperatures requires trapping at pressures higher than 130 MPa. As a consequence we think that it is reasonable to hypothesize trapping pressures of about 200 MPa for these fluids (7-8 km of depth assuming lithostatic pressure). This suggestion is in agreement with estimated pressure of contact metamorphism (150-200 MPa) in the hornfels rocks (Carella et al., 2000) and is comparable with depth of emplacement for other Neogene intrusions and magma chambers in southern Tuscany (Ruggieri and Lattanzi, 1992; Maineri, 1996; Marianelli and Carletti, 1999; Mazzarini et al., 2004; Dini et al., 2005; Rossetti et al., 2007; Fulignati in prep., Table 2). Type 3a hypersaline fluid inclusions could be therefore considered as representative of the first fluids exsolved from the granitic body, during its rise in the upper crust, under lithostatic pressure of about 200 MPa. On the other hand, the early direct exsolution of a magmatic hypersaline fluid phase from Cl-bearing granitic magmas has been widely demonstrated by several authors (Cline and Bodnar, 1991; Webster, 1997, 2004). The temperatures (about 430 °C) estimated in Figure 6, assuming 200 MPa of trapping pressure, are merely indicative and probably underestimated because the investigated fluid inclusions are far more complex than pure H₂O-NaCl brine as a consequence the topology of the diagram changes, as pointed out by Kodera et al. (2004). Another possibility to explain the behaviour of brines entrapped within Type 3a fluid inclusions is that they were produced by aqueous fluid immiscibility. To evaluate this possibility we considered a fluid with a salinity of 40 wt% NaCl generated by immiscibility at a pressure of 110 MPa (corresponding to the lithostatic pressure at about 4150 m of depth and an average density of the overlying rocks of 2600 kg/m³). Experimental data of Bodnar et al. (1985) indicate that a liquid with a salinity of 40 wt% NaCl_{equiv} will be produced through immiscibility at 110 MPa, at temperatures of about 690 °C, along the liquid-vapour

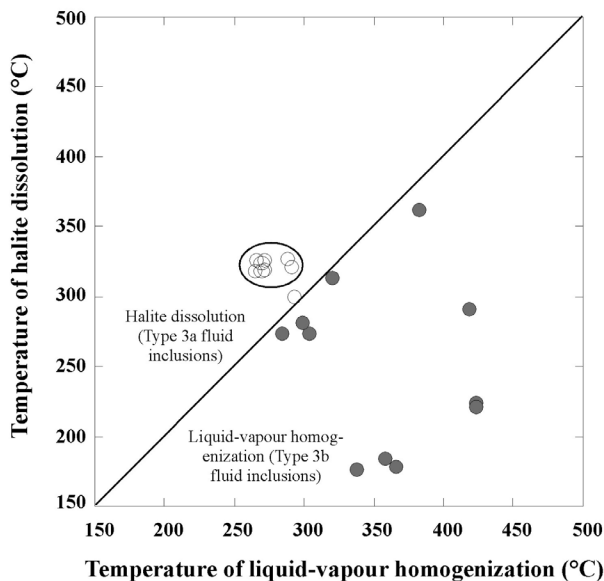


Figure 5. Liquid-vapour homogenization temperature (T_h) vs. halite dissolution temperature (T_s) for Type 3 fluid inclusions. The oval is traced to identify the densest cluster, which is assumed to represent best the fluid trapped in Type 3a fluid inclusions.

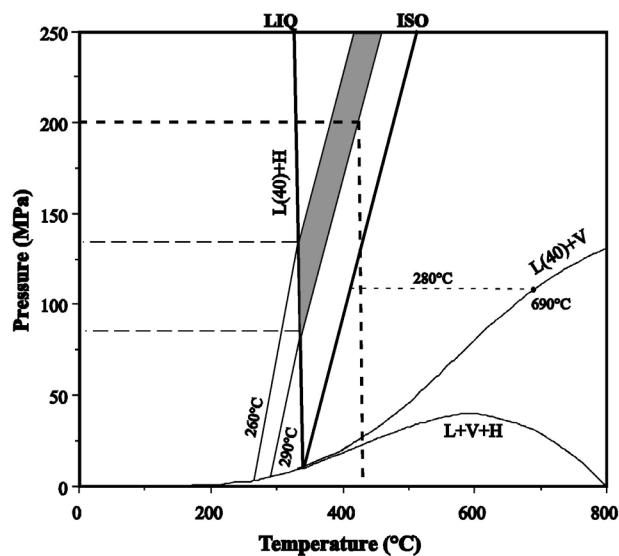


Figure 6. Temperature-pressure diagram of part of the NaCl-H₂O system, illustrating trapping conditions for the dense cluster of data points (see Figure 5) representing Type 3a fluid inclusions that exhibit average liquid-vapour homogenization at 260° and 290 °C and that undergo final homogenization by halite dissolution at 305 °C and 335 °C. The diagram shows the liquid + vapour + NaCl curve (L+V+H), the liquid + vapour curve (L+V) and corresponding liquidus (L+H) for 40 wt% NaCl_{equiv}. The intersection of the iso- T_h lines and the [L(40)+H] liquidus defines the minimum trapping pressure and temperature for the fluid in Type 3a fluid inclusions.

curve for a 40 wt% NaCl_{equiv} fluid (Figure 6). To produce inclusions that homogenize by halite dissolution, the 690 °C fluids must have been isobarically cooled about 280 °C, prior to trapping (Figure 6). This is unlikely because this would imply that fluid temperature would have been uniformly reduced by 280 °C prior to trapping of any fluid inclusions. Inclusions trapping fluids at 600-690 °C and 110 MPa of pressure would homogenize to the liquid phase at temperatures ranging between about 550° and 690 °C (Bodnar and Vityk, 1994) and we did not find any Type 3 inclusions homogenizing above 440 °C. Furthermore, vapour-rich inclusions coexisting with Type 3a inclusions were never observed. Thus, we consider that Type 3a fluids are best interpreted as being generated directly by separation of brine from a water-saturated crystallizing silicate melt.

As stated before, petrographic evidences suggest that Type 3b postdate Type 3a fluid inclusions. Type 3b fluid inclusions, showing final homogenization by vapour-bubble disappearance, could therefore represent a later stage of magmatic fluid evolution. According to Cline and Bodnar (1994), these inclusions were trapped in the portion of the liquid-stable region between the isochore (ISO) and the liquid-vapour curve (L(40)+V). As a consequence, these fluids could have existed stably as a single phase or coexisted with a vapour phase, but the absence of coexisting vapour-rich fluid inclusions strongly supports the first hypothesis. The fair decrease in salinity,

Table 2. Estimated depth of emplacement of Neogene magmatic bodies of southern Tuscany.

	Pressure of emplacement (MPa)	References
Larderello (Travale 1sud well)	~200	This work
Campiglia M.ma	>90	1
Mt. Capanne (Elba Island)	150-200	2, 3
Giglio Island	200-250	4
Roccastrada	150-180	5
Gavorrano	~150	6

1 Fulginati in prep.; 2 Ruggieri and Lattanzi (1992); 3 Rossetti et al. (2007); 4 Maineri (1996); 5 Marianelli and Carletti (1999); 6 Mazzarini et al. (2004).

shown by Type 3b fluid inclusions, might be interpreted in terms of dilution of magmatic brines by low-salinity external fluids. In this case, these inclusions would record the initial inflow of meteoric fluids in the system with subsequent mixing with magmatic fluids, following the ductile to brittle transition of reholological environment.

Meteoric water-dominated hydrothermal (geothermal) stage

The infiltration of surficial fluids of meteoric origin in the hydrothermal system, following the transition from lithostatic to hydrostatic pressure conditions, is suggested by Type 1 and Type 2 fluid inclusions that record the development of the meteoric water-dominated geothermal system that is still active. The temperatures recorded by Type 1a and Type 2 inclusions are higher than the present-day temperature at the depth of sampling (Figure 7). This suggests a cooling of the system with time. At 3017m of depth, Type 1a and Type 2 fluid inclusions have very similar T_h . This might suggest the occurrence of boiling processes, but no clear evidence regarding the coexistence of this Type of inclusions with liquid-rich ones was observed. Type 2 inclusions furthermore display a wide range of salinity that reaches values too high for a vapour produced by boiling. However, assuming a boiling process, these high salinities may be partly due to the

entrapment of some small amount of liquid with the vapour phase. In this case, the salinity determined in the vapour rich inclusions would not represent the composition of the vapour phase present at trapping but, rather, some salinity intermediate between the liquid and vapour composition (Bodnar and Vityk, 1994). Furthermore, T_h and T_{mi} measurements of vapour rich inclusion are usually inaccurate because it is difficult to accurately determine homogenization and final melting temperature when only small quantities of liquid are present. Taking into account all these elements, the occurrence of boiling processes at 3017 m of depth remains ambiguous and we cannot support it unequivocally.

Type 1b fluid inclusion population displays T_h close to the present-day temperatures either at 3017 m and 4150 m of depth (Figure 7), analogously to what observed in other fluid inclusion studies on Larderello geothermal system (Ruggieri et al., 1999; Ruggieri and Bertini, 2000; Boyce et al., 2003). Taking into account a relatively low pressure of formation (under hydrostatic or vaporstatic conditions) for these inclusions, we assumed that T_h approximates the trapping temperatures. For these reasons, these fluid inclusions can be considered as representative of the geothermal fluid actually circulating in the granite.

CONCLUSIVE REMARKS

Fluid inclusion investigation on a granite intrusion cored by the Trav. 1s geothermal well, located in the eastern sector of Larderello high-enthalpy geothermal field, took in evidence that the first fluids circulated in the system were generated by direct exsolution of a magmatic hypersaline brine by the crystallizing melt. This probably occurs during the late stage of magma rise in the upper crust, under lithostatic pressure of about 200 MPa. These results clearly testify, for the first time at Larderello, the evolution of hypersaline magmatic fluids from crystallizing granite magma, and are in agreement with what hypothesized by Valori et al. (1992) and Cathelineau et al. (1994) in the western sector of the geothermal field. In fact, they proposed that the brines, which they found as fluid inclusions in hornfels and dykes from the deeper portions of the geothermal system, were thought to have been expelled from an underlying granite intrusion.

Type 3a and 3b multiphase fluid inclusions, which homogenize by halite disappearance and vapour bubble disappearance respectively, record the progressive release of magmatic fluids from the crystallizing granite magma, with Type 3b inclusions that may record the initial inflow of meteoric fluids in the system with subsequent mixing with magmatic fluids, following the ductile to brittle transition.

Two-phase (Type 1 and Type 2) inclusions are representative of the hydrothermal meteoric water-

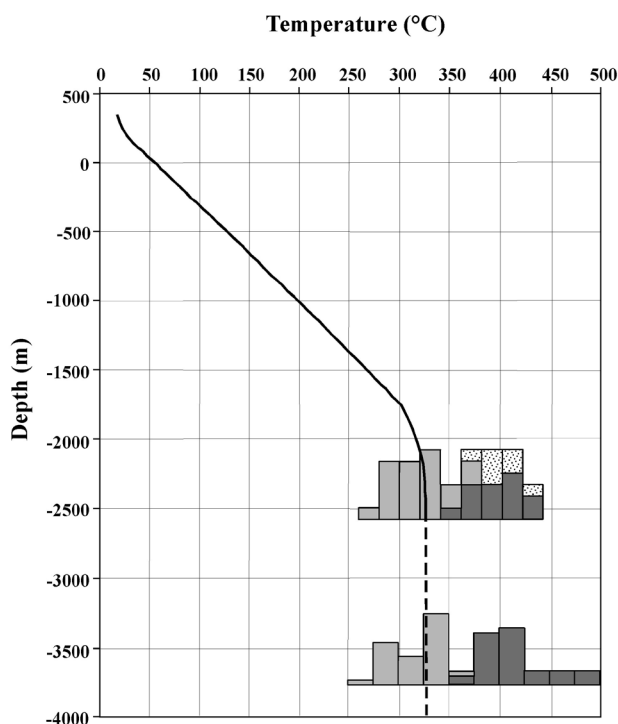


Figure 7. Temperature of homogenization of Type 1 and Type 2 fluid inclusions and thermal profile comparison for Trav. 1s geothermal well (legend as Figure 4).

dominated fluids that penetrated in the granite after opening of the system, induced by cooling and consequent transition from ductile behaviour to brittle fracturing. Fluid inclusion data show a general cooling of the system. In this view, Type 1b fluid inclusions, having temperature of homogenization that agree well with down-hole measured temperatures, may be considered to approximate the fluid that is actually circulating in the granite in recent times.

ACKNOWLEDGEMENTS

I am grateful to Giovanni Ruggieri for his helpful comments and suggestions on an early version of the manuscript. Many thanks are also due to an anonymous reviewer whose suggestions improved the quality of the manuscript, and to Prof. Castorina for editorial handling.

REFERENCES

- Baldi P., Bellani S., Ceccarelli A., Fiordelisi A., Rocchi G., Squarci P., Taffi L., 1995. Geothermal anomalies and structural features of southern Tuscany (Italy). *Proceedings of World Geothermal Congress, Florence*, 2, 1287-1291.
- Barelli A., Bertini G., Buonasorte G., Cappetti G., Fiordelisi A., 2000. Recent deep exploration results at the margins of the Larderello Travale geothermal system. *Proceedings of World Geothermal Congress, Kyushu, Japan*, 965-970.
- Belkin H.E., De Vivo B., Gianelli G., Lattanzi P., 1985. Fluid inclusions in minerals from the geothermal fields of Tuscany, Italy. *Geothermics* 14, 59-72.
- Bertini G., Casini M., Gianelli G., Pandeli E., 2006. Geological structure of a long-living geothermal system, Larderello, Italy. *Terra Nova* 18, 163-169.
- Bodnar R.J., 1993. Revised equation and table for determining the freezing point depression of H₂O-NaCl solutions. *Geochimica et Cosmochimica Acta* 57, 683-684.
- Bodnar R.J., 1994. Synthetic fluid inclusions XII. The system H₂O-NaCl: Experimental determination of the liquidus and isochors for a 40 wt% H₂O-NaCl solution. *Geochimica et Cosmochimica Acta* 58, 1053-1063.
- Bodnar R.J. and Vityk M.O., 1994. Interpretation of microthermometric data for H₂O-NaCl fluid inclusions. In: B. De Vivo, M.L. Frezzotti (eds.), *Fluid Inclusions in Minerals: Methods and Applications*, pp. 117-130.
- Bodnar R.J., Burnham C.W., Sterner S.M., 1985. Synthetic fluid inclusions in natural quartz III. Determination of phase equilibrium properties in the system H₂O-NaCl to 1000 °C and 1500 bars. *Geochimica et Cosmochimica Acta* 49, 1861-1873.
- Boiron M.C., Cathelineau M., Ruggieri G., Jeanningros A., Gianelli G., Banks D.A., 2007. Active contact metamorphism and CO₂-CH₄ fluid production in the Larderello geothermal field (Italy) at depths between 2.3 and 4 km. *Chemical Geology* 237, 303-328.
- Boyce A.J., Fulignati P., Sbrana A., 2003. Deep hydrothermal circulation in a granite intrusion beneath Larderello geothermal area (Italy): constraints from mineralogy, fluid inclusions and stable isotopes. *Journal of Volcanology and Geothermal Research* 126, 243-262.
- Carella M., Fulignati P., Musumeci G., Sbrana A., 2000. Metamorphic consequences of Neogene thermal anomaly in the northern Apennines (Radicondoli - Travale area, Larderello geothermal field - Italy). *Geodinamica Acta* 13, 345-366.
- Cathelineau M., Marignac C., Boiron M.C., Gianelli G., Puxeddu M., 1994. Evidence for Li-rich brines and early magmatic fluid-rock interaction in the Larderello geothermal system. *Geochimica et Cosmochimica Acta* 58, 1083-1099.
- Cline J.S. and Bodnar R.J., 1991. Can economic porphyry copper mineralization be generated by a typical calc-alkaline melt? *Journal of Geophysical Research* 96, 8113-8126.
- Cline J.S. and Bodnar R.J., 1994. Direct evolution of brine from a crystallizing silicic melt at the Questa, New Mexico, molybdenum deposit. *Economic Geology* 89, 1780-1802.
- Crawford M.L., 1981. Phase equilibria in aqueous fluid inclusions. In: L.S. Hollister and M.L. Crawford (eds.), *Short Course in Fluid Inclusions: Application to Petrology*. Mineralogical Association of Canada 6, 75-100.
- Dini A., Gianelli G., Puxeddu M., Ruggieri G., 2005. Origin and evolution of Pliocene-Pleistocene granites from the Larderello geothermal field (Tuscan Magmatic Province, Italy). *Lithos* 81, 1-31.
- Gianelli G., Manzella A., Puxeddu M., 1997. Crustal models of the geothermal areas of southern Tuscany (Italy). *Tectonophysics* 281, 221-239.
- Goldstein R.H., 2003. Petrographic analysis of fluid inclusions. In: I. Samson, A. Anderson, D. Marshall (eds), *Fluid Inclusions: Analysis and Interpretation*. Mineralogical Association of Canada Short Course 32, 9-53.
- Goldstein R.H. and Reynolds T.J., 1994. Systematics of fluid inclusions in diagenetic minerals. *Society for Sedimentary Geology Short Course* 31, pp. 1-199.
- Hedenquist J.W. and Henley R.W., 1985. The importance of CO₂ on freezing point measurements of fluid inclusions: evidence from active geothermal systems and implication for epithermal ore deposition. *Economic Geology* 80, 1379-1406.
- Kodera P., Lexa J., Rankin A.H., Fallick A.E., 2004. Fluid evolution in a subvolcanic granodiorite pluton related to Fe and Pb-Zn mineralization, Banská Stianica ore district, Slovakia. *Economic Geology* 99, 1745-1770.
- Maineri C., 1996. Magmatic-hydrothermal system of the Isola del Giglio granitoid intrusion, Southern Tuscany. *Plinius* 15, 103-108.
- Marianelli P. and Carletti P., 1999. Genesis of Roccastrada volcanic rocks (central Italy): inferences from melt inclusions analyses. *Periodico di Mineralogia* 68, 69-80.
- Marinelli G., 1963. L'energie geothermique en Toscane. *Annales Société Géologique Belgique* 85, 417-438.

- Marinelli G., Barberi F., Cioni R., 1993. Sollevamenti Neogenici e intrusioni acide della Toscana e del Lazio Settentrionale. *Memorie della Società Geologica Italiana* 49, 279-288 in Italian with English abstract
- Mazzarini F., Corti G., Musumeci G., Innocenti F., 2004. Tectonic control on laccolith emplacement in northern Apennines fold-thrust belt: The Gavorrano intrusion (southern Tuscany, Italy). *Physical Geology of High-Level Magmatic Systems*. Breitkreuz C. and Petford N. (eds.) Geological Society Special Publication 234, 151-161.
- Mongelli F., Palumbo F., Puxeddu M., Villa I.M., Zito G., 1998. Interpretation of the geothermal anomaly of Larderello, Italy. *Memorie della Società Geologica Italiana* 52, 305-318.
- Roedder E., 1984. Fluid inclusions. *Reviews in Mineralogy* 12, pp.646.
- Rossetti F., Tecce F., Billi A., Brilli M., 2007. Patterns of fluid flow in the contact aureole of the late Miocene Monte Capanne pluton (Elba Island, Italy): the role of structures and rheology. *Contribution to Mineralogy and Petrology* 153, 743-760.
- Ruggieri G. and Lattanzi P., 1992. Fluid inclusion studies on Mt. Capanne pegmatites, Isola d'Elba, Tuscany, Italy. *European Journal of Mineralogy* 4, 1085-1096.
- Ruggieri G. and Gianelli G., 1999. Multi-stage fluid circulation in a hydraulic fracture breccia of the Larderello geothermal field (Italy). *Journal of Volcanology and Geothermal Research*, 90, 241-261.
- Ruggieri G. and Bertini G., 2000. The use of fluid inclusions for temperature estimations in the Larderello geothermal field (Italy). *Proc. of World Geothermal Congress, Kyushu, Japan, May 28-June 10, 2815-2819*.
- Ruggieri G., Cathelineau M., Boiron M.C., Marignac C., 1999. Boiling and fluid mixing in the chlorite zone of the Larderello geothermal system. *Chemical Geology* 154, 237-256.
- Serri G., Innocenti F., Manetti P., 1993. Geochemical and petrological evidence of the subduction of delaminated Adriatic continental lithosphere in the genesis of the Neogene-Quaternary magmatism of central Italy. *Tectonophysics* 223, 117-147.
- Shepherd T.J., Rankin A.H., Alderton D.H.M., 1985. A practical guide to fluid inclusion studies. Blackie, Glasgow and London, pp.239.
- Shinohara H., Iiyama J.T., Matsuo S., 1989. Partition of chlorine compounds between silicate melt and hydrothermal solutions: I. Partition of NaCl-KCl. *Geochimica et Cosmochimica Acta* 53, 2617-2630.
- Steele-MacInnis M., Lecumberri-Sanchez P., Bodnar R.J., 2012. HOCKIEFLINCS-H2O-NACL: A Microsoft Excel spreadsheet for interpreting microthermometric data from fluid inclusions based on the PVTX properties of H₂O-NaCl. *Computer Geoscience* 49, 334-337.
- Sterner S.M., Hall D.L., Bodnar R.J., 1988. Synthetic fluid inclusions. V. Solubility relations in the system NaCl-KCl-H₂O under vapor-saturated conditions. *Geochimica et Cosmochimica Acta* 52, 989-1006.
- Valori A., Cathelineau M., Marignac C., 1992. Early fluid migration in a deep part of the Larderello geothermal field: a fluid inclusion study of the granite sill from well Monteverdi 7. *Journal of Volcanology and Geothermal Research* 51, 115-131.
- Villa I.M., Ruggieri G., Puxeddu M., 1997. Petrological and geochronological discrimination of two mica generations in a granite cored from the Larderello-Travale geothermal field (Italy). *European Journal of Mineralogy* 9, 563-568.
- Webster J.D., 1997. Exsolution of magmatic volatile phases from Cl-enriched mineralizing granitic magmas and implications for ore metal transport. *Geochimica et Cosmochimica Acta* 61, 1017-1029.
- Webster J.D., 2004. The exsolution of magmatic hydrosaline chloride liquids. *Chemical Geology* 210, 33-48.



This work is licensed under a Creative Commons Attribution 4.0 International License CC BY. To view a copy of this license, visit <http://creativecommons.org/licenses/by/4.0/>

